

RSC Advances

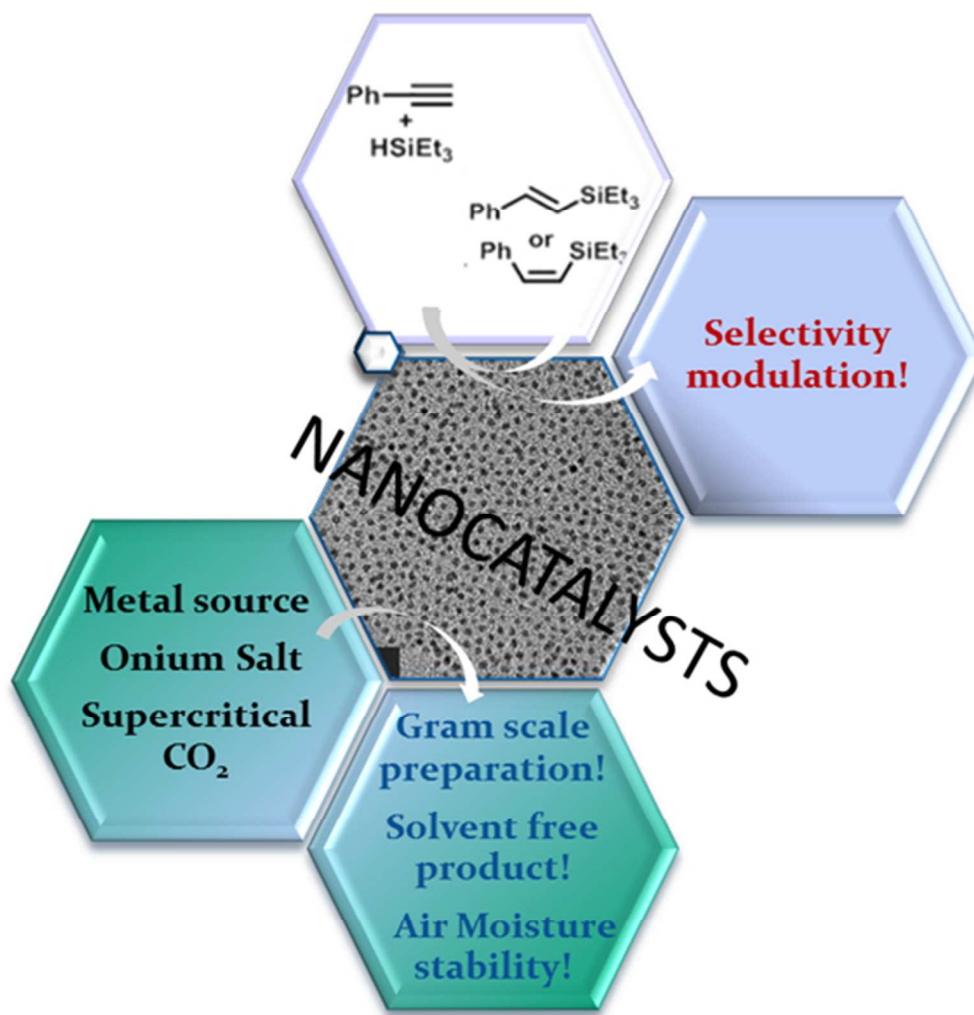


This is an *Accepted Manuscript*, which has been through the Royal Society of Chemistry peer review process and has been accepted for publication.

Accepted Manuscripts are published online shortly after acceptance, before technical editing, formatting and proof reading. Using this free service, authors can make their results available to the community, in citable form, before we publish the edited article. This *Accepted Manuscript* will be replaced by the edited, formatted and paginated article as soon as this is available.

You can find more information about *Accepted Manuscripts* in the [Information for Authors](#).

Please note that technical editing may introduce minor changes to the text and/or graphics, which may alter content. The journal's standard [Terms & Conditions](#) and the [Ethical guidelines](#) still apply. In no event shall the Royal Society of Chemistry be held responsible for any errors or omissions in this *Accepted Manuscript* or any consequences arising from the use of any information it contains.



152x154mm (96 x 96 DPI)

ARTICLE

Cite this:
10.1039/x0xx00000xDOI: **Catalysed stereodivergent hydrosilylation with Onium Salts stabilised M(0) Nanocatalysts prepared in scCO₂**Received 00th January 2012,
Accepted 00th January 2012O. Pascu,^a V. Liautard,^b M. Vaultier,^b M. Pucheault^{*,b} and C. Aymonier^{*,a}

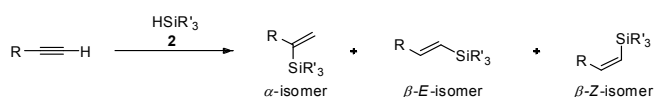
DOI: 10.1039/x0xx00000x

www.rsc.org/

M(0) nanocatalysts stabilised in Onium Salt were synthesised using an original preparation and their effectiveness to catalyse the challenging selective stereodivergent alkyne hydrosilylation reaction was studied. Four metal based nanocrystals, namely Pt, Ir, Rh and Ru stabilised by three Onium Salts (quaternary ammonium salts with different anions and cations), were successfully prepared by supercritical CO₂ assisted synthesis. The Onium salts with three different structures were chosen considering their effect on nanocrystals morphology and surface properties but without interference in the selectivity towards hydrosilylation reaction. It was found that the stereochemical outcome can be adjusted either by varying the metal but preserving the same Onium Salt stabilizer, or varying the metal NCs surface properties by changing the stabilizer structure.

Introduction

Transition metal catalysed hydrosilylation reaction is a major challenge for silicone industry. To date, the most efficient olefin hydrosilylation catalysts¹ are platinum complexes. Triple bond hydrosilylation, as it affords vinylsilanes as powerful building blocks, has attracted a lot of attention in organic synthesis. However, the terminal alkynes hydrosilylation is considered as challenging since they usually yield a hardly separable mixture of three isomers, α -, β -(*E*) and β -(*Z*) (Scheme 1). In homogeneous catalysis, it was found that product distribution could be adjusted by i) using a metal (neutral or cation) with specific stereoelectronic properties, ii) selecting a proper metal-ligand combination or iii) playing with the reaction parameters. However, all these routes have the drawback of being very laborious, time consuming and sometimes even more expensive.

**Scheme 1** Hydrosilylation of terminal alkynes

Since Lewis³ reported that platinum “colloids” can be involved in the hydrosilylation mechanism, opening the way to heterogeneous hydrosilylation catalysis, various supported platinum catalysts have been used such as Pt/C,⁴ Pt/SiO₂,⁵

Pt/TiO₂⁶ and PtO₂⁷. More recently gold as Au/TiO₂⁸, AuNPore⁹, Rh/GNF¹⁰ and lately palladium¹¹ as heterogeneous catalysts have been also employed. However, even with the few successfully reports on selective alkyne hydrosilylation in the presence of transition-metal heterogeneous catalysts,² their main deficiency is not only the limitation in catalyst choice, restricted to a handful of supports (e.g. carbon, silica, oxides) in association with a dozen of metals but also to the lack of a proper catalyst design and characterisation (e.g. morphology, surface properties, organization) for a better understanding of their catalytic behaviour. Moreover, the cheap large scale synthesis of stable and sustainable nanocatalysts owning a high specific surface area is still under investigation.

Thus, the challenge and an increased interest rely in the design of advanced and highly efficient catalytic systems with properties for selectivity oriented hydrosilylation. Yet, to our knowledge, only few examples with particular focus on catalyst design and its physicochemical properties study have been reported. For example, hydrosilylation regioselectivity could be controlled in a confined environment using nanoreactors made of graphitized carbon nanofibres (GNF) embedded with 3 nm Rh or RhPt NPs.¹⁰ In addition, it was found that within the nanoreactor, the NPs size, loading and NPs surfactant's surface coverage did not effect notably the product distribution, while the reactants stoichiometry, the balance of aliphatic and aromatic moieties seemed to be more important.

In this paper, we explore alkyne hydrosilylation reaction using M(0) nanocatalysts stabilised with Onium Salt (OS). In order to obtain a catalyst that can perform stereodivergent hydrosilylation reaction we have chosen to use i) four metals (Pt, Ir, Rh and Ru), already known to afford different selectivities in homogeneous systems.¹⁻² Indeed, platinum catalysts are assumed to lead to β -*E* isomers through a modified Chalk-Harrod mechanism,¹² while for Ru, Rh and Ir, Crabtree and Ojima reported an alternative mechanism which could eventually afford the thermodynamically disfavoured β -*Z* isomer.¹³ We also used ii) Quaternary ammonium salts (OS) as surface stabilizer with a more likely influence on NPs surface properties but without interferences as ligands toward hydrosilylation regiochemical outcome (being almost inert and working mainly as transfer agent).

A series of nanocatalysts has been prepared using a modification of the synthetic approach previously developed by our group.^{14,15} Metal nanocrystals (NCs) synthesis in Ionic Liquids (ILs) mediated by supercritical CO₂ (scCO₂) was chosen as adequate route for our objectives. ILs are attractive compounds not only as solvent and stabilizers¹⁶ but also as reducing agents¹⁷. Although the Room Temperature Ionic Liquids are the most used, other Onium Salts (OS), with higher melting point (above 100 °C), and very scarcely studied because of their high melting point,¹⁵ shall be considered in this study since at supercritical conditions their melting point is considerable decreased. These compounds used in scCO₂ environment could play an important role in designing advanced hybrid organic-inorganic NCs¹⁸ opening thus new avenues for catalytic chemical reactions¹⁵ or materials synthesis.^{19,20} Additionally, the solvent free preparation-assisted by scCO₂ of M(0) NCs¹⁹ affords, in the absence of any additional organic solvent, hybrid organic-inorganic ready-to-use dry powder catalysts, containing highly crystalline metal NCs, free from any undesired organic parts²⁰.

To assess the role of OS on NCs physicochemical properties (size, shape, surface chemistry, organisation) three different Onium Salts have been chosen (Figure 1): one with a high melting point, namely cetyltrimethylammonium bromide (CTAB, m.p. of 250 °C), used as a reference and other two with lower melting points, tetrabutylammonium bromide (TBAB, m.p. 102 °C) and cetyltrimethylammonium bis(trifluoromethylsulfonyl)imide (CTANTf₂, m.p. 84 °C) changing the cation and the anion, respectively from the reference salt). Special focus is given to the effect of nanocatalysts morphology and surface properties on the catalytic behaviour, which is evaluated in this work by terminal alkyne hydrosilylation reaction.

Experimental

Generalities

The metal precursors were purchased from Sigma-Aldrich and Strem Chemicals and used as received: ruthenium (III) acetylacetonate (Ru(acac)₃, 97%), rhodium (II) trifluoroacetate dimer (Rh(tfa)₃, 95%), chloro-1,5-cyclooctadiene iridium (I)

dimer ([Ir(cod)Cl]₂, 99%) and platinum (II) hexafluoroacetylacetonate (Pt(hfac)₂, 98%). The quaternary ammonium salts TBAB and CTAB were purchased from Sigma-Aldrich. Cetyltrimethylammonium bis(trifluoromethylsulfonyl)imide (CTANTf₂, m.p. of 84 °C) was prepared according to a reported methodology.²¹ Phenylacetylene and triethoxysilane were purchased from Alfa Aesar and used as received.

All catalytic reactions were carried out under argon atmosphere. ¹H NMR was recorded on Bruker Avance 300 FT 300 MHz spectrometers using CDCl₃ as internal reference. Chemical shifts (δ) and coupling constants (*J*) are expressed in ppm and Hz, respectively. The following abbreviations were used to report multiplicities: s = singlet, d = doublet, t = triplet, q = quartet, m = multiplet. GC-MS analysis were performed on an HP 6890 series GC-system equipped with a J&W Scientific DB-170 capillary column, an HP 5973 mass selective detector (EI) using the following method: 70 °C for 1 min then 20 °C min⁻¹ until 230 °C then 6 min at 230 °C.

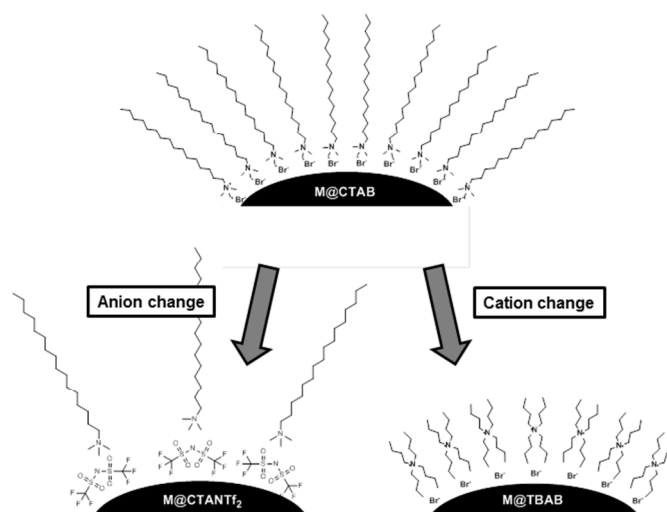


Figure 1. Sketch of the hybrid organic-inorganic NCs catalysts namely metal (0) stabilized by Onium Salts (OS) labeled as M@CTAB (the reference), M@TBAB, and M@CTANTf₂, where M = Pt, Ir, Rh and Ru

Nanocatalyst preparation

For the synthesis in supercritical fluid media, a home-made high pressure/high temperature stirred batch reactor with a stainless steel cell, and a volume of 60 mL was used. Within the reactor, the white powder quaternary ammonium salts were mixed with the metal precursor (1% wt metal) also in powder form (Figure 2). 3.4 bar of CO₂+H₂ gas mixture in molar ratio 80:20 were first loaded from a gas bottle and afterward pressurized to the desired pressure (230 bar) with CO₂ through a high pressure pump. The pressure inside the reactor was monitored with a pressure sensor. The reaction temperature (100 ≤ T ≤ 185 °C) was controlled by an external heating element surrounding the reactor and a thermocouple placed inside the reactor. After 30 minutes, the reactor was depressurized and CO₂ vented through the reactor for few more minutes. The final product, nanoparticles embedded in the solid

matrix of ammonium salt was recovered as dark powder (Figure 2) and used directly in hydrosilylation.



Figure 2. Synthesis procedure for the preparation of metal nanocrystals stabilized in the solid matrix of ammonium salts, labeled M@OS NCs.

Following the experimental parameters listed below, and focusing on commonly employed metal salt,²⁰ we prepared original nanostructured materials (Table 1).

²⁰**Table 1.** Precursors and reaction temperatures used for the preparation of M@OS nanocatalysts were OS = CTAB, TBAB, and CTANTf₂ and M = Pt, Ir, Rh and Ru.

Precursor type T _r °C	scCO ₂ -230 bar / 30 min		
	TBAB	CTAB	CTANTf ₂
Ru(acac) ₃ 185°C	Ru@TBAB	Ru@CTAB	Ru@CTANTf ₂
Rh(tfa) ₃ 150°C	Rh@TBAB	Rh@CTAB	Rh@CTANTf ₂
[Ir(cod)Cl] ₂ 100 and 185°C	Ir@TBAB	Ir@CTAB	Ir@CTANTf ₂
Pt(hfac) ₂ 100 and 185°C	Pt@TBAB	Pt@CTAB	Pt@CTANTf ₂

Materials Characterization

Final materials morphologies, labelled M@TBAB, M@CTAB and M@CTANTf₂, respectively (M = Ru, Rh, Ir and Pt) were characterized by conventional (TEM-JEOL 2100) and high resolution (TEM-FEG HR-JEOL 2200FS) transmission electron microscopy. Samples were prepared by dissolving the powdered hybrid nanocatalyst in an organic solvent and depositing it by drop casting onto a carbon grid. Toluene was our first choice as solvent, due to the good solubilisation of Onium Salts, but unfortunately due to the presence of high amounts of organics on the grid, nanocrystals could not be clearly seen. By changing the solvent to ethanol or acetone, better images were obtained at the expense of NCs agglomeration. Powder XRD analysis on the above mentioned

systems were performed using an X-ray diffractometer with Cu $\lambda_{K\alpha}$ radiation (PANanalytical X'Pert Pro). For FTIR reflection measurements a Bruker spectrophotometer working in the range 7500-400 cm⁻¹ was used.

General procedure for phenylacetylene hydrosilylation

Triethoxysilane (1.0 mmol) and then phenylacetylene (1.0 mmol) were added under Argon to a 15 mL reaction tube containing the M@OS (0.1 mol%). The reaction mixture was stirred at 85°C for 23h. After reaction, dichloromethane was added to the reaction mixture followed by filtration over a pad of silica. After washing twice with 10 mL of dichloromethane the filtrate was concentrated under vacuum to give the corresponding vinyl silane as a mixture of isomers. Product distribution was determined by GC/MS using the relative areas of products. Conversion was determined using the relative areas of phenylacetylene in GC/MS and comparing to mesitylene as internal standard.

Triethoxy(1-phenylvinyl)silane 3a^{3,6}: ¹H NMR (300 MHz, CDCl₃) δ 7.58-7.11 (m, 5H), 6.16 (d, 1H, *J* = 3 Hz), 5.97 (d, 1H, *J* = 3 Hz), 3.83 (q, 6H, *J* = 7 Hz), 1.21 (t, 9H, *J* = 7 Hz); MS (EI) *t*_R = 7,81 min; *m/z*: 135 (71%), 163.1 (33%), 222 (100%), 266.1 (M⁺, 8%).

(*Z*)-Triethoxy(styryl)silane 3b⁶: ¹H NMR (300 MHz, CDCl₃) δ 7.58-7.11 (m, 6H), 6.18 (d, 1H, *J* = 19.5 Hz), 3.89 (q, 6H, *J* = 7 Hz), 1.27 (t, 9H, *J* = 7 Hz); MS (EI) *t*_R = 8,70 min; *m/z*: 147 (71%), 176,1 (61%), 222 (100%), 251.1 (50%), 266.1 (M⁺, 9%).

(*E*)-Triethoxy(styryl)silane 3c¹²: ¹H NMR (300 MHz, CDCl₃) δ 7.65-7.15 (m, 6H), 5.59 (d, 1H, *J* = 15.6 Hz), 3.76 (q, 6H, *J* = 7 Hz), 1.15 (t, 9H, *J* = 7 Hz); MS (EI) *t*_R = 8,12 min; *m/z*: 222 (M+H-OEt, M⁺, 100%).

Triethoxy(phenylethyl)silane 5¹³: MS (EI) *t*_R = 8,56 min; *m/z*: 147 (63%), 163 (84%), 205 (100%), 235.1 (71%), 264.1 (M⁺, 81%).

Results and discussion

Metal effect.

As mentioned in the introduction, the goal of this work was to explore the stereodivergent hydrosilylation reaction using new hybrid system-M(0) NCs stabilized in OS. Prior to assessing catalysts selectivities, the physicochemical properties of the nanocatalysts were studied to better understand their catalytic behaviour.

Metal NCs formation is based on metal precursor reduction with H₂ mediated by scCO₂ only in the presence of Onium Salts. The scCO₂ environment together with the melted Onium Salt¹⁹ play the solvent role for the precursor dissolution, and decomposition into its metal form formation; the present case being in good agreement with our previous report.^{14,15} It is expected that different OSs will have an influence on NCs morphology such as, size, shape, organisation and perhaps surface properties. TEM images of M(0) stabilised by the reference CTAB (label M@CTAB) are presented in Figure 3.

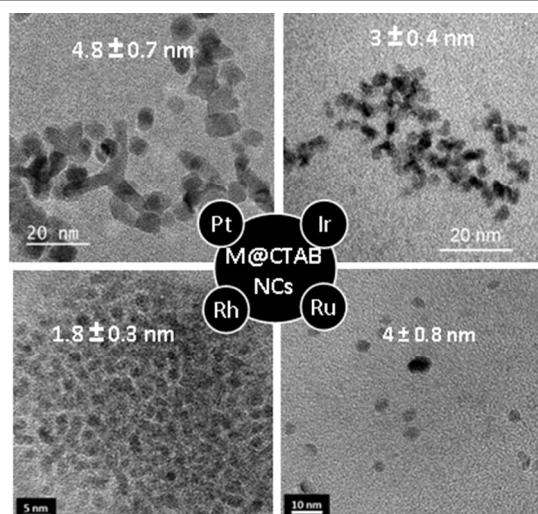
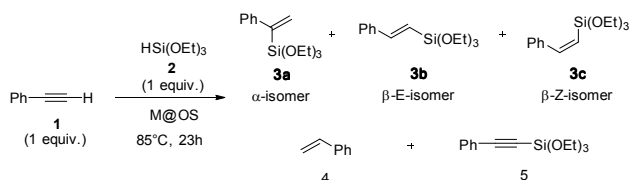


Figure 3. TEM images of the 4 metal types stabilised by high m.p. CTAB, taken as our reference system, with the NCs sizes obtained from a Gaussian distribution by counting more than 150 NCs.

As already known, depending on the metal type, NCs size and shape could vary when using the same stabiliser. Larger NCs and with an isotropic growth tendency were obtained for Pt, showing a difference in precursor decomposition kinetics and nucleation & growth regime. CTAB structure, a dissymmetric alkyl chains with one chain having more than twelve carbon atoms, might also favour the NCs growth. It was reported^{18a,19a} that this kind of structures could behave as liquid crystals upon melting, translated in an increased mobility of its long alkyl chain prompt to bend easily. Reorganization and chains flexibility will influence nanocrystals formation, allowing for a higher metal atoms movement along the metal nuclei thus resulting in their higher growth (Figure 3). Their different organization, well dispersed for Ru, more agglomerated for Pt and Rh and aggregated for Ir, reflects their different surface properties and implicitly different catalytic behaviour. After the study of nanocatalysts morphology and surface properties, we evaluated the catalytic behaviour of M@CTAB NCs.

To address regio- and stereoselectivity points resulting from addition across the C≡C triple bond, we used phenylacetylene, a terminal alkyne, affording three possible isomers (Scheme 2). Triethoxysilane was chosen as the silylating agent since the obtained vinyl triethoxysilane is relatively stable; the resulting vinylsiloxane being classical cross coupling partner. Moreover, it is less acidic than triethylsilane, hence less reactive, being thus a better choice for comparison. As mentioned earlier,² hydrosilylation reaction may be catalysed by various metals (Pt, Ir, Rh and Ru), although Speier's and Karstedt's homogeneous Pt catalysts remain the most efficient.



Scheme 2. Reaction conditions for terminal alkyne hydrosilylation catalyzed by M@OS NCs.

For this reason, we carried out preliminary experiments using the Pt@OS NCs and an equimolar ratio of phenylacetylene and triethoxysilane. Of the three OS, we took cetyltrimethylammonium bromide (CTAB) as reference stabiliser which has the higher melting point. When 0.1 mol% (metal content) of catalyst was used, we were pleased to find that the expected β -E-isomer **3b** was obtained at 85°C as major product (Table 2, entry 1). In agreement with previously reported platinum heterogeneous hydrosilylation no β -Z-isomer **3c** was observed³⁻⁸ and the regioselectivity is close to that obtained with homogeneous industrial catalysts such as Speier's (entry 2) and Karstedt's catalyst (entry 3) leading to 23-30% of α isomer.

Table 2. Comparison of selectivity between Pt@CTAB, Speier's and Karstedt's catalyst.

Entry	Catalyst (mol%)	Product distribution (%)				Select ^a (%)	Yield (%)
		α	β -E	β -Z	4		
1	Pt@CTAB (0.1)	30	64	0	0	68	86
2	H ₂ PtCl ₆ (0.5)	23	75	2	0	75	100
3	Karstedt (0.1)	25	75	0	0	75	93

Alkyne (1 equiv.), silane (1 equiv.), 85°C, 23h were used in all reactions.^a Proportion of major isomer.

Encouraged by our preliminary results with Pt@CTAB we prepared and tested in catalysis original Ir, Ru and Rh analogs. Interestingly, even though homogeneous ruthenium complexes have shown high levels of selectivity, little attention has been paid to their heterogeneous counterparts in the literature. In the actual study and as predicted, Pt@CTAB was the only one providing mainly the β -E isomer (Table 3). In contrast, for the aggregated Ir@CTAB and smaller size Rh@CTAB the selectivity was lower and in favour of the β -Z isomer obtained in poor yields. These are in agreement with Ir and Rh NCs morphology and surface properties, discussed above. It is worth noticing that when hydrosilylation was carried out with Ru@CTAB good yield and β -Z selectivity were reached, again in good agreement with our expectations.

Table 3. Phenylacetylene hydrosilylation using the hybrid systems M@CTAB with their corresponding product distribution.

Entry	M@CTAB	Product distribution (%)					Select ^a	Yield (%)
		1	α	β -E	β -Z	4		
1	Pt@CTAB	6	30	64	0	0	68	86
2	Ir@CTAB	86	1	4	4	5	51	43
3	Rh@CTAB	73	2	4	9	12	60	45
4	Ru@CTAB	15	3	20	51	10	68	81

Alkyne (1 equiv.), silane (1 equiv.), 85°C, 23h were used in all reactions.^a Proportion of major isomer.

Temperature influence on nanocatalysts synthesis.

Another aspect of catalyst preparation which could affect NCs surface properties and thus catalytic performance is NCs synthesis temperature. Both Ir@CTAB and Pt@CTAB NCs were prepared at two different temperatures, 100 and 185 °C respectively and keeping all the other experimental parameters constant. The reaction temperature is affecting reaction kinetics and implicitly NCs nucleation and growth.²⁰ As expected and reported previously²², a faster kinetics gave rise to a burst nucleation and smaller NCs formation. This scenario fits very well for Ir NCs, but less for Pt. At 100 °C, Ir NCs are obtained with a mean size of 3 nm (Figure 3) decreasing to around 1.7 nm at 185 °C (Figure 4b). In the case of Pt, the NCs synthesized either at 185 (Figure 4a) or 100 °C (Figure 3) show two populations of morphologies: for both temperatures, monodispersed rounded shape with square tendency of 5 nm size NCs (Figures 3 and 4a inset) are obtained representing the majority. A smaller population displayed an isotropic growth, stars at 100 °C (Figure 3) or 4 leaf clover type at 185 °C (Figure 4a). These unexpected morphologies could influence the Pt NCs catalytic behaviour as various crystal faces are displayed on the surface. FTIR measurements (Figure 4c) were performed for both Ir and Pt NCs at both reaction temperatures in order to verify if the stabilizer CTAB changed or preserved its chemical structure influencing the NCs properties. No significant changes were observed suggesting the preservation of the Onium Salt structure and properties after the scCO₂ treatment. However, we do not rule out the possibility that during NCs synthesis, CTAB organization, as thermotropic liquid crystals,^{18a,19a} is changing thus influencing the NCs isotropic growth.

Regarding catalytic activity, both metal NCs prepared at higher reaction temperature displayed an important reaction yield drop (Table 4) as a consequence of their different morphology and surface properties.

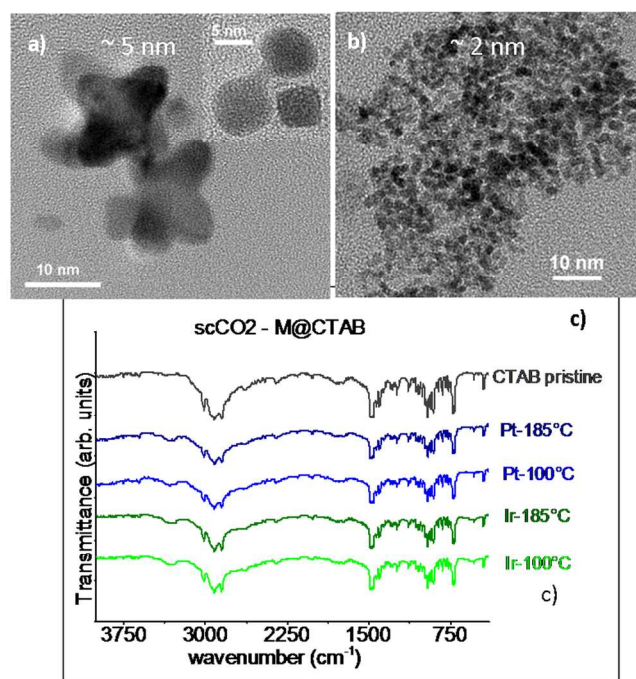


Figure 4. TEM images of Pt@CTAB (a) and Ir@CTAB (b) system prepared at 185°C reaction temperatures with their mean size obtained from the Gaussian size distribution. FTIR spectra of Ir and Pt@CTAB, at the two synthesis temperatures, in comparison with pristine CTAB (c).

Table 4. Influence of the M@CTAB NCs temperature synthesis on catalytic activity for two systems.

Entry	M@OS	Product distribution (%)					Yield (%)
		1	α	β -E	β -Z	4	
1	Ir@CTAB ^a	86	4	4	1	5	43
2	Ir@CTAB ^b	100	0	0	0	0	0
3	Pt@CTAB ^a	6	30	64	0	0	86
4	Pt@CTAB ^b	44	8	23	0	25	59

Alkyne (1 equiv.), silane (1 equiv.), 0.1% catalyst, 85°C, 23h were used in all reactions.^a M@OS was prepared at 100°C.^b M@OS was prepared at 185°C.

Stabilizer effect on nanocatalysts properties

As pointed out earlier, NCs properties can be modified by changing the stabilizer type and structure (Figure 1). Using TBAB, with a bulkier (shorter and symmetric) cation and CTANTf₂, with a different anion, both OS having relatively low melting point, allowed us to evaluate the stabilizer effect (Figure 5). The smallest sizes, down to 2 nm, for all metals (Pt, Ir, Rh and Ru) were obtained when using TBAB (Figures 1 and 5-left column). As previously observed,²³ ligands displaying different electronic, steric and binding strength to metal centre, affects NCs size, morphology and time stability. By using a bulkier stabilizer, a dense, compact shell around the metal core could be formed, preventing attachment from other coming metal atoms and thus maintaining a small size for the NCs. This

growth mechanism can match the present situation with M@TBAB system.

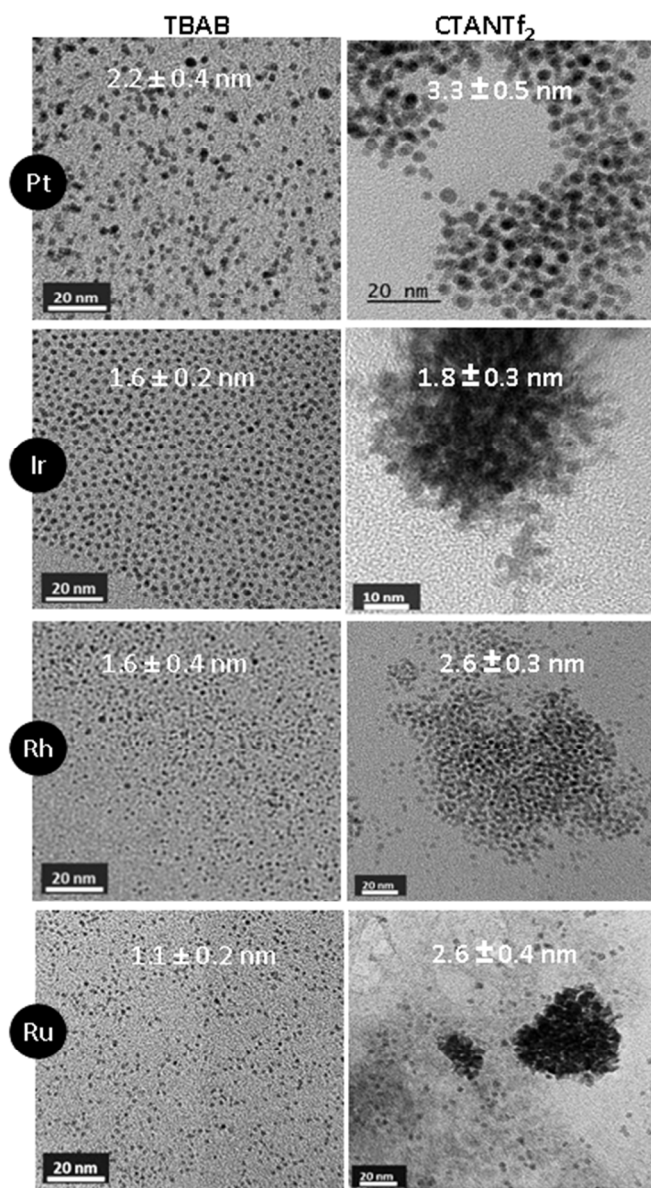


Figure 5. TEM images of the hybrid systems M@TBAB (left column) and M@CTANTf₂ (right column) with their corresponding sizes obtained from a Gaussian distribution

By changing the OS anion part, from bromide to bis(trifluoromethylsulfonyl)imide (NTf₂) (Figure 5 right column), a clear influence on NCs size, shape and organization was revealed. Pt NCs went from a square to a smaller rounder shape with good size and shape monodispersity. Ir and Rh maintained their organization type but with size change. The more surprising stabilizer effect is for Ru, large aggregation and size decrease being observed. We assume that the presence of oxygen atoms in the anion, could have the ability to coordinate to the surface metal atoms, as a bidentate or a polydentate ligand, forming perhaps a thin oxide layer, unfortunately not

visible by HRTEM analysis, which might inactivate the NCs surface. Another factor that should be taken in consideration is the corroboration of local electronic densities of both metal and anion which might affect NCs surface properties. It is worth noticing that reported supercritical media assisted synthesis results only in highly crystalline materials. This is proved by surface area electron diffraction (SAED) analysis of HRTEM micrographs (Figure 6) and the NCs lattice fringe clearly seen.

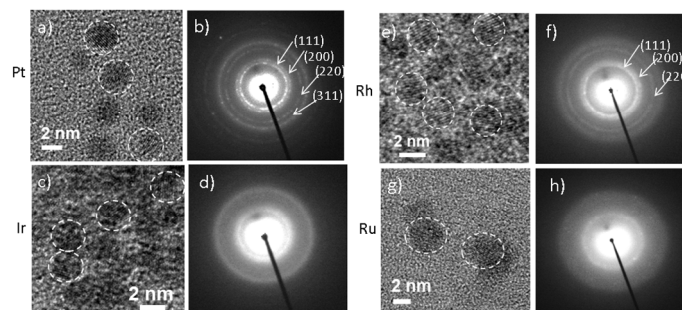


Figure 6. HRTEM (a,c,e,g) and SAED (b,d,f,h) images corresponding to the systems M@OS given the best catalysis results: Pt@TBAB (a,b), Ir@TBAB (c,d), Rh@TBAB (e,f) and Ru@CTAB (g,h).

Indeed, the NPs size is not the only factor influencing the catalytic activity (Table 5). While small and monodispersed M@TBAB NCs reacts efficiently for Pt, Ir and Rh providing high conversion, the M@CTANTf₂ system was found to be less active, being linked maybe to the NCs surface properties in the presence of NTf₂ anion.

Table 5. Phenylacetylene hydrosilylation using the hybrid systems M@OS with their corresponding product distribution.

Entry	M@OS	Product distribution (%)					Select ^a	Yield (%)
		1	<i>α</i>	<i>β-E</i>	<i>β-Z</i>	4		
1	Pt@TBAB ^b	0	23	67	1	0	76	100 ^c
2	Pt@CTANTf ₂	45	23	32	0	0	58	70
3	Ir@TBAB	16	16	36	32	0	43	84
4	Ir@CTANTf ₂	81	3	13	2	0	71	54
5	Rh@TBAB ^c	62	2	8	28	0	73	73
6	Rh@CTANTf ₂	57	0	11	7	25	63	68
7	Ru@TBAB	46	2	6	46	-	86	45
8	Ru@CTANTf ₂	100	-	-	-	-	-	0

Alkyne (1 equiv.), silane (1 equiv.), 0.1% catalyst, 85°C, 23h were used in all reactions. ^a Proportion of major isomer. ^b 9% of PhC≡CSi(OEt)₃ **5** were also formed. ^c Catalyst loading 0.01%.

As expected, for all OS, Pt NCs provided good *β-E* selectivity and less than 1% of *β-Z* isomer (Table 5, entries 1-2). More sterically hindered cation, TBAB, allows us to reach homogeneous complexes (Speier and Karstedt) yields and selectivity (Tables 2 and 5). However, when the nature of the Onium Salt anion changed from bromide to NTf₂ the *β-E/α* selectivity decreased (Table 5, entry 2). Other metals NCs led

to unfavored β -Z isomer formation, while limiting the formation of the α -isomer. Neutral homogeneous Rh catalysts are known to lead to Z-vinylsilanes.²⁴ In our case nonetheless, depending on the Onium Salt, Rh NCs afforded predominantly either the β -Z or β -E isomer and a small amount of α isomer (Table 5, entries 5-6). Rh@TBAB afforded better yields and selectivity (for β -Z isomer, Table 5, entry 5). In contrast by using a long chain Onium Salt (Table 3, entry 3 and Table 5, entry 6) increased significantly styrene proportion, formed by hydrosilylation. One can notice that Rh@CTANTf₂ led to β -E isomer predominantly albeit in poor yield (Table 5, entry 6). Unfortunately among all Ru@OS prepared (Table 3, entry 4 and Table 5, entries 7-8), only Ru@CTAB seems to be efficient in the selected hydrosilylation reaction, allowing the formation of 68% of β -Z isomer and only traces of α (Table 3, entry 4). Moving to a triflimide counter anion annihilates the reaction whereas using TBAB led to a lower conversion albeit in an excellent 86% of β -Z selectivity (Table 5, entry 7). More surprising was the way Onium Salt affects the selectivity for Ir NCs. Indeed, even if Ir@TBAB was the most active NCs, it also led to the lowest selectivity. For example, the Ir NCs stabilization with CTANTf₂ led to a mixture of the 3 isomers in a 1/4/1 ratio (Table 5, entry 4), instead of 1/2/2 with TBAB (Table 5, entry 3).

Table 6. Nanocatalysts loading: Pt@TBAB in phenylacetylene hydrosilylation.

Entr y	Pt@TBA B ppm	Product distribution (%)					Yiel d (%) ^b	
		1	α	β -E	β -Z	4		5
1	10	85	4	5	0	0	6	11
2	100	0	26	71	0	0	3	100
3	1,000	0	23	67	1	0	9	100
4	10,000	0	5	60	3	0	32	100

Alkyne (1 equiv.), silane (1 equiv.), 85°C, 23h were used in all reactions.

Nanocatalyst concentration

We finally explored the concentration effect on the hydrosilylation carried out with our most powerful catalyst, namely Pt@TBAB. Unsurprisingly, it was observed a significant dependence on the selectivity/NCs concentration. The more nanocatalyst was used, the more by-product was formed (Table 6). While decreasing the amount of NCs to 100 ppm has limited the formation of side products including β -E isomer (Entry 2), the further decrease to 10 ppm Pt@TBAB afforded a lower conversion and a similar amount of α -3, β -E-3 and 5 (Entry 1). The latter product is formally resulting from the direct dehydrogenative coupling between 1 and 2, but can also originate from the β -elimination of a putative vinyl-platinum intermediate complex.

Conclusions

By this work, we presented a novel nanocatalysts design based on transition metal nanocrystals stabilized by Onium Salts. The preparation approach, scCO₂ assisted synthesis, not only afford direct powdered, ready-to-use, air/moisture stable nanocatalyst, but also highly active hydrosilylation catalyst free from any undesired organics. Pt@TBAB allowed us to perform efficient selective β -E hydrosilylation of phenylacetylene using only 10 ppm of NC, to date one of the most efficient heterogeneous nanocatalyst. With a particular focus on nanocatalysts morphology and surface properties, to better understand NCs catalytic behaviour, we have presented the implications of some experimental parameters on nanocatalysts efficiency. By using advanced hybrid organic-inorganic NCs we successfully made a step toward hydrosilylation stereoselectivity modulation by: i) varying the metal but preserving the same Onium Salt stabilizer; ii) varying the metal NCs morphology and surface properties by changing either the stabilizer structure (different anion or cation) or NCs synthesis temperature and iii) varying NCs concentration with direct effect on nanocatalysts selectivity. It is worth noticing that this approach led to the first examples of selective β -Z hydrosilylation catalyzed by Ruthenium nanocatalyst.

With further optimization on nanocatalysts surface properties, for example using additional ligands, lower reaction yields obtained for some M@OS systems, can be overcome.

Acknowledgements

The authors want to acknowledge the financial support to the Aquitaine Region and the ANR-12-CDII-010-NANOCAUSYS.

Notes and references

a CNRS, Université de Bordeaux, ICMCB, UPR 9048, F-33600 Pessac, France. Dr Cyril Aymonier, ICMCB-CNRS, 87 avenue du Dr Albert Schweitzer, 33608 Pessac Cedex, France. Email: aymonier@icmcb-bordeaux.cnrs.fr

b CNRS, Université de Bordeaux, ISM, UMR 5255, F-33405 Talence, France. Dr Mathieu Pucheault, ISM, 351 cours de la libération 33405 Talence Cedex, France. Email: m.pucheault@ism.u-bordeaux1.fr

References

1. B. Marciniec, Functionalisation and Cross-Linking of Organosilicon Polymers. In *Hydrosilylation*, Marciniec, B., Ed. Springer Netherlands: 2009; Vol. 1, pp 159-189.
2. B. Marciniec, Hydrosilylation of Alkynes and Their Derivatives. In *Hydrosilylation*, B. Marciniec, Ed. Springer Netherlands: 2009; Vol. 1, pp 53-86.
3. L. N. Lewis, *Chem. Rev.* 1993, **93**, 2693-2730.
4. M. Chauhan, B. J. Hauck, L. P. Keller and P. J. Boudjouk, *Organomet. Chem.*, 2002, **645**, 1-13.
5. R. Jimenez, J. M. Martinez-Rosales and J. Cervantes, *Can. J. Chem.*, 2003, **81**, 1370-1375.
6. F. Alonso, R. Buitrago, Y. Moglie, J. Ruiz-Martinez, A. Sepúlveda-Escribano and M. Yus, *Organomet. Chem.*, 2011, **696**, 368-372.
7. A. Psyllaki, I. N. Lykakis and M. Stratakis, *Tetrahedron*, 2012, **68**, 8724-8731.

ARTICLE

8. A. Hamze, O. Provot, J.-D. Brion, M. Alami, *Synthesis* 2007, 2025-2036; R. Cano, M. Yus, D. J. Ramón, *ACS Catalysis* 2012, **2**, 1070-1078.
9. Y. Ishikawa, Y. Yamamoto, N. Asao, *Catal. Sci. Technol.* 2013, **3**, 2902-2905.
10. W. A. Solomonsz, G. A. Rance, M. Suyetin, A. La Torre, E. Bichoutskaia and A. N. Khlobystov, *Chem. – Eur. J.*, 2012, **18**, 13180-13187.
11. M. Planellas, W. Guo, F. Alonso, M. Yus, A. Shafir, R. Pleixats, T. Parella, *Adv. Synth. Catal.* 2014, **356**, 179-188.
12. A. J. Chalk and J. F. Harrod, *J. Am. Chem. Soc.*, 1967, **89**, 1640-1647.
13. C.-H. Jun and R. H. Crabtree, *Organomet. Chem.*, 1993, **447**, 177-187; I. Ojima, N. Clos, R. J. Donovan, P. Ingallina, *Organometallics* 1990, **9**, 3127-3133.
14. S. Moisan, V. Martinez, P. Weisbecker, F. Cansell, S. Mecking and C. Aymonier, *J. Am. Chem. Soc.*, 2007, **129**, 10602-10606.
15. F. Hassine, M. Pucheault and M. Vaultier, *Comptes Rendus Chimie*, 2011, **14**, 671-679. 16. J. D. Scholten, B. C. Leal and J. Dupont, *ASC Catal.* 2012, **2**, 184-200; C. Vollmer and C. Janiak, *Coord. Chem. Rev.*, 2011, **255**, 2039-2057.
17. W. Darwich, C. Gedig, H. Srour, C. C. Santini and M. H. G. Prechtel, *RSC Adv.*, 2013, **2**, 20324-20331; C.-H. Pelisson, C. Hubert, A. Denicourt-Nowicki, A. Roucoux, *Top Catal.* 2013, **56**, 1220-1227.
18. (a) A. M. Scurto, E. Newton, R. R. Weikel, L. Draucker, J. Hallet, Ch. L. Liotta, W. Leitner, Ch. A. Eckert, *Ind. Eng. Chem. Res.* 2008, **47**, 493-501. (b) F. Jutz, J.-M. Andanson, A. Baiker, *Chem. Rev.* 2011, **111**, 322-353. (c) S. V. Dzyuba, R. A. Bartsch, *Angew. Chem. Int. Ed.* 2003, **42**, 148-150.
19. (a) S. G. Kazarian, N. Sakellarios and Ch. M. Gordon, *Chem. Comm.*, 2002, 1314; (b) V. Cimpeanu, M. Kocevar, V. I. Parvulescu and W. Leitner, *Angew. Chem. Int. Ed.*, 2009, **48**, 1085-1088.
20. (a) S. E. Bozbag, D. Sanli and C. Erkey, *J. Mater. Sci.* 2012, **47**, 3469-3492; (b) F. Cansell and C. Aymonier, *J. Supercrit. Fluids*, 2009, **47**, 508-516.
21. H. D. S. Guerrand, L. D. Marciasini, T. Gendrineau, O. Pascu, S. Marre, S. Pinet, M. Vaultier, C. Aymonier, M. Pucheault, *Tetrahedron*, 2014, **70**, 6156-6161.
22. S. Marre, A. Erriguible, A. Perdomo, F. Cansell, F. Marias and C. Aymonier, *J. Phys. Chem. C.*, 2009, **113**, 5096-5104.
23. O. Pascu, L. Marciasini, S. Marre, M. Vaultier, M. Pucheault and C. Aymonier, *Nanoscale*, 2013, **5**, 12425-12431.
24. A. Mori, E. Takahisa, Y. Yamamura, T. Kato, A. P. Mudalige, H. Kajiro, K. Hirabayashi, Y. Nishihara and T. Hiyama, *Organometallics*, 2004, **23**, 1755-1765.